Structure and mode of action of the antimicrobial peptide arenicin

Jörg Andrä*[1], Igor Jakovkin[†], Joachim Grötzinger[†], Oliver Hecht[‡], Anna D. Krasnosdembskaya[§], Torsten Goldmann*, Thomas Gutsmann*, and Matthias Leippe[‖]

*Research Center Borstel, Leibniz-Center for Medicine and Biosciences, Parkallee 10, 23845 Borstel, Germany

[†]Institute of Biochemistry, Christian-Albrechts-University, Olshausenstr. 40, 24098 Kiel, Germany

[‡]School of Chemical Science and Pharmacy Stores, University of East Anglia, NR47TJ Norwich, UK

[§]Department of Histology and Cell Biology, St. Petersburg State University, Universitetskaya nab. 7/9, 199034 St. Petersburg, Russia

[‖]Department of Zoophysiology, Zoological Institute, Christian-Albrechts-University, Olshausenstr. 40, 24098 Kiel, Germany

Abbreviations: AMP, antimicrobial peptide; CFU, colony forming unit; FRET, Förster resonance energy transfer; LPS, lipopolysaccharide; MIC, minimal inhibitory concentration; MBC, minimal bactericidal concentration; PC, phosphatidylcholine; DPhyPC, Diphytanoyl-PC; PE, phosphatidylethanolamine; PG, phosphatidylglycerol; NBD-PE, N-(7-nitrobenz-2-oxa-1,3-diazol-4yl)-PE; Rh-PE, rhodamin-PE.

[1]**Corresponding author:** Jörg Andrä, Immunochemistry and Biochemical Microbiology, Research Center Borstel, Leibniz-Center for Medicine and Biosciences, Parkallee 10, 23845 Borstel, Germany, Tel. 49-4537-188280; fax 49-4537-188632; Email: jandrae@fz-borstel.de

Synopsis

The solution structure and the mode of action of arenicin isoform 1, an antimicrobial peptide with a unique 18-residue loop structure, from the lugworm *Arenicola marina* were elucidated here. Arenicin folds into a two-stranded anti-parallel β-sheet. It exhibits high antibacterial activity at 37°C and 4°C against Gram-negative bacteria, including polymyxin B resistant *Proteus mirabilis*. Bacterial killing occurs within minutes and is accompanied by membrane permeabilisation, membrane detachment, and release of cytoplasm. Interaction of arenicin with reconstituted membranes that mimic the lipopolysaccharide-containing outer membrane or the phospholipid-containing plasma membrane of Gram-negative bacteria exhibited no pronounced lipid specificity. Arenicin-induced current fluctuations in planar lipid bilayers correspond to the formation of short lived heterogeneously structured lesions. Our data strongly suggest that membrane interaction plays a pivotal role in the antibacterial activity of arenicin.

Keywords: antimicrobial peptide, atomic force microscopy, epithelial defence, lipopolysaccharide, membrane permeabilisation, planar lipid bilayer

Short title: Mode of action of the cyclic antimicrobial peptide arenicin

INTRODUCTION

Two isoforms of a new class of antibacterial cationic peptides, termed arenicins, have been recently isolated from the coelomocytes of the marine polychaeta lugworm, *Arenicola marina* [1]. The mature peptides consist of 21 amino-acid residues comprising a disulfide bond, and a unique 18 amino-acid residue loop structure. They are rich in arginine and hydrophobic amino-acid residues (Tyr and Trp) and differ only by a single, conservative amino acid substitution (V10I). Both isoforms exhibit indentical potent antimicrobial activity against *Escherichia coli*, *Listeria monocytogenes*, and *Candida albicans* [1]. Due to their molecular size, net charge and origin, arenicins are classified as natural antimicrobial peptides (AMPs), also referred to as host defence peptides [2,3]. This expanding group of peptides forms a part of the innate immune system of all animals. They are secreted by specific immune cells, such as neutrophils [4], NK-cells, or coelomocytes [5], and are also found on exposed body surfaces, e.g. skin and lung, where they provide a first line of defence against invading pathogens [6-8]. These peptides display a highly diverse tertiary structure. Prominent examples are linear α-helical peptides such as magainins [9] and cecropins [10], or β-sheet structures with a complex disulfide pattern, e.g. the defensins [4,11]. The arenicin structure, however, appears to be unique. As arenicins bear a net positive charge (+6) in combination with a substantial number of hydrophobic amino-acid residues, a membranolytic step involved in the killing of microorganism may be assumed. However, information on the the arenicin-membrane interaction is incomplete and the mechanism of the antibiotic action remains elusive.

Here, we present a comprehensive study on the mode of action of this extraordinary peptide with a focus on Gram-negative bacteria. Using NMR spectroscopy, we elucidated the solution structure of arenicin isoform 1 (RWCVYAYVRVRGVLVRYRRCW-COOH), and investigated and visualized its interaction with viable bacteria possessing defined lipopolysaccharide structures and with the corresponding reconstituted membrane mimetics. This study included determination of the biological activity of arenicin, an ultrastructural analysis of arenicin-treated bacteria by atomic force microscopy and electron microscopy, permeabilisation of bacterial membranes, elucidation of the different steps of arenicin´s membrane interaction, i.e. binding, insertion and permeabilisation using FRET spectroscopy, arenicin-mediated dissipation of the membrane potential of liposomes, and electrical measurements of arenicin-induced lesions in planar lipid bilayers.

EXPERIMENTAL

Peptides, phospholipids, and reagents

Chemically synthesized arenicin (RWCVYAYVRVRGVLVRYRRCW-COOH) with a non-amidated C-terminus was purchased from Biosyntan GmbH (Berlin, Germany). The sequence is identical to that of arenicin isoform-1, which differs from isoform 2 by a single amino acid substitution (V10I), as previously identified [1] and is referred to throughout this manuscript as arenicin. The correct formation of the disulfide linkage (Cys3-Cys20) of the synthetic peptide was confirmed by mass spectrometry (kindly performed by C. Gelhaus). Melittin was synthesized by solid phase synthesis by Fmoc chemistry and purified by HPLC as described previously [12]. Asolectin and polymyxin B, in its sulfate salt form, were purchased from Sigma (Deisenhofen, Germany). Phospholipids, cardiolipin, 1,2-diphytanoyl-*sn*-glycero-3-phosphocholine (DPhyPC, synthetic), L-α-phosphatidylcholine (PC, chicken egg), L-α-phosphatidyl-DL-ethanolamine (PE, *E. coli*), L-α-phosphatidyl-DL-glycerol (PG, chicken egg) were purchased from Avanti Polar Lipids (Alabaster, AL, USA). Lipids (purity >99%) were used without further purification. N-(7-nitrobenz-2-oxa-1,3-diazol-4yl)-phosphatidyl-ethanolamine (NBD-PE) and N-(lissamine rhodamine B sulfonyl)-phosphatidyl-ethanolamine (Rh-PE) were from Molecular Probes (Eugene, OR, USA). All other chemicals were analytical grade and purchased from Merck (Darmstadt, Germany).

Bacteria and bacterial culture

The bacterial strains used were six Gram-negative and one Gram-positive isolate: i) Deep rough mutant strains with defined LPS Re structures (Fig. 1): *Escherichia coli* WBB01, *Salmonella enterica* Sv Minnesota R595, *Proteus mirabilis* R 45, ii) strains with the complete LPS core sugar (LPS Ra): *E. coli* ATCC 23716, *S. enterica* Sv Minnesota R60, iii) *E. coli* K-12 strain D31, an ampicillin- and streptomycin-resistant strain, the lipopolysaccharide core of which lacks some glucose, galactose and rhamnose residues [13], and iv) a Gram-positive representative, *Bacillus megaterium* (ATCC 14581). Bacteria were grown overnight in Luria-Bertani (LB) medium with constant shaking at 37 °C and subsequently inoculated in the same medium to reach the mid-logarithmic phase.

Lipopolysaccharide

Deep-rough type lipopolysaccharide (LPS) was extracted from *E. coli* strain WBB01 grown at 37 °C by the phenol/chloroform/petrol ether method, purified, and lyophilized [14].

NMR experiments and structure calculation

Arenicin (1.8 mg) was dissolved in 0.7 ml of 88% H_2O/10% D_2O/2% (v/v) deuterated acetic acid. Two-dimensional TOCSY (τ_m=75ms) and NOESY (τ_m=150ms) spectra with WATERGATE solvent suppression were recorded on a Varian Inova 600 MHz Spectrometer at 283.15 K. Hydrogen bonding was evaluated using H-D exchange experiments. Hydrogen bonds were detected by recording one-dimensional ^{1}H-spectra after dissolving 1.8 mg arenicin in D_2O; hydrogen bonds were assigned only to amide protons that still were detectable after 16 h. The assignment of proton resonances was carried out using TOCSY and NOESY data. Interproton distance restraints were derived from the cross-peak intensities in the NOESY spectrum by $1/r^6$ – calibration. Additional distance restraints were added to represent the Cys3-Cys20 disulfide bond and hydrogen bonds in the peptide backbone. Structure calculations were performed with the CYANA 2.1 program [15] applying a simulated annealing-molecular dynamics protocol. Five hundred structures were calculated and the 10 structures with the lowest target function were chosen to represent the ensemble and to calculate the average structure. For graphical representation the RIBBONS and Grasp software was used [16,17].

Assay for hemolytic activity

Twenty µl of washed human erythrocytes (5 x 10^8 cells/ml) in 10 mM phosphate-buffered saline, pH 7.4, were incubated with 80 µl of a peptide sample in the same buffer for 30 min at 37°C or 4°C in a round bottom microtiter plate (Nunclon Surface, Nunc, Roskilde, Denmark). After the incubation period the plate was centrifuged at 1000 x g for 10 min to remove intact erythrocytes, and the concentration of released hemoglobin was measured in a microtiter plate reader at 405 nm (Rainbow, Tecan, Grödig/Salzburg, Austria) after ten-fold dilution of the supernatant. Hemolytic activity was expressed as percent hemolysis (% hemolysis = $((OD_{Sample}-OD_{buffer})/(OD_{max}-OD_{buffer})*100)$. Maximal lysis ($OD_{max}$) was achieved by adding distilled water instead of the peptide sample to the cells. Data shown represent the mean of at least two experiments each performed in duplicate.

Assay for cytotoxic activity

The influence of peptides on the viability of human cells was determined by monitoring the increase of the fluorescence of alamarBlue (BioScource) caused by metabolically active cells only. Jurkat cells were grown in RPMI 1640 medium (GIBCO-BRL) supplemented with 10 % fetal bovine serum (PAA-laboratories, Parkerford, USA) at 37°C and 5% CO_2, washed twice in 20 mM MES, 150 mM NaCl, pH 5.5 and resuspended in the same buffer. Five x 10^5 cells (40 µl) were added to two-fold serial dilutions of the proteins in the same buffer (50 µl) in a precoated microtiter plate (0.1 % bovine serum albumin (Sigma-Aldrich) at 20°C for 10 min) and incubated at 37°C and 5% CO_2. After 30 min, 10 µl of alamarBlue (final concentration: 10 %) were added and the cells were incubated for another 30 min. The increase of fluorescence was measured in the microtiter plate fluorescence spectrophotometer (Fluoroskan II, Labsystems) using an excitation wavelength of 538 nm and an emission wavelength of 590 nm. The fluorescence difference between Jurkat cells treated with 0.1 % Triton-X100 and cells treated with buffer only under the same conditions was taken as the value for 100 % cytotoxic activity. Peptide concentrations at which 50 % of the cells were killed (LD_{50}) were derived from dose-response curves. Each curve represents the mean of two independent experiments, each performed in duplicate.

Assays for antibacterial activity

a) Determination of minimal inhibitory and bactericidal concentrations

Peptides were dissolved in the indicated buffer (Table 1). Each solution (180 µl) was pipetted into the first well of a microtiter plate. For a two-fold serial dilution, 90 µl of each solution was transferred to the next well filled with the same volume of buffer. Subsequently, a suspension of log-phase bacteria in LB medium was added (10 µl, containing 10^4 colony forming units, CFU) to each peptide solution (90 µl). The plates were incubated overnight in a wet chamber at 37°C (or 4°C when indicated) with constant shaking and bacterial growth was monitored by measuring the absorbance at 620 nm in a microtiter plate reader (Rainbow, Tecan, Crailsham, Germany). The minimal inhibitory concentration (MIC) was defined as the lowest peptide concentration, at which no bacterial growth was measurable. Portions of each well (10 µl) were diluted with buffer, plated out in duplicate on LB-agar plates, incubated overnight at 37°C, and bacterial colonies were counted. The minimal bactericidal concentration (MBC) was defined as the peptide concentration where no colony growth was observed. The values were expressed as the mean of at least two independent experiments, each performed in duplicate, with a divergence of not more than one dilution step.

b) Time course of bacterial killing

(25 µl) and 2 µM of the fluorescent dye SYTOX Green (25 µl; in 10 mM Hepes, 25 mM NaCl, pH 7.4) at 37 °C for 1 h. Permeabilisation of the bacterial outer and /or cytoplasmic membrane allows the dye to cross the membranes and to intercalate into the DNA. When excited at 495 nm, the binding of the dye to DNA resulted in an increase of emitted fluorescence at 538 nm which was measured in a microtiter plate reader (Fluoroskan II; Labsystems, Milford, MA, USA). Membrane-permeabilizing activity of the peptides was expressed as percentage of permeabilized bacteria. For maximum permeabilisation of the bacteria (100% value), cells were incubated with 70% ethanol for 5 min. The values were expressed as the mean of two independent experiments, each performed in duplicate.

Circular dichroism (CD) spectroscopy

CD measurements were carried out on a Jasco J-720 spectropolarimeter (Japan Spectroscopic Co., Ltd., Tokyo, Japan), calibrated according to [18]. CD spectrum measurement represents the average of at least three scans obtained by collecting data at 1 nm intervals with a bandwidth of 2 nm. The measurements were performed in 50 mM sodium phosphate, pH 5.8, at 10°C in a 1.0 cm tandem quartz cuvette. The two chambers of the tandem cuvette were filled with either the peptide solution or the liposome suspension, respectively. After recording the CD-spectrum the cuvette was shaken for 20 min in order to mix the peptide solution and liposome suspension and a second CD-spectrum was recorded. The ratio of arenicin and PG was 0.85:1 (w/w).

Förster resonance energy transfer (FRET) spectroscopy

Intercalation of arenicin into phospholipid liposomes and LPS aggregates was determined at indicated temperatures by FRET spectroscopy applied as a probe-dilution assay as described earlier [19]. The peptide was added to the liposomes (suspended in 20 mM Hepes, 150 mM NaCl, pH 7.0), and intercalation was monitored as the increase of the quotient between the donor fluorescence intensity I_D at 531 nm and the acceptor intensity I_A at 593 nm (FRET signal) in dependence of time. All measurements were performed at least twice with no major discrepancies. Representative curves are shown.

Assay for pore-forming activity

Pore-forming activity of arenicin was determined by measuring fluorimetrically the dissipation of a valinomycin-induced membrane potential in asolectin liposomes [20]. The measurements were repeated eight times and a representative curve is shown.

Preparation of planar bilayers and electrical measurements

Planar lipid bilayers were prepared according to the Montal-Mueller technique [21] as described earlier in detail [22,23]. For the reconstitution of the cytoplasmic membrane of human cells, instead of natural PC, DPhyPC was used to obtain a higher stability of the membranes. The inner leaflet of the outer membrane of Gram-negative bacteria was reconstituted by a phospholipid mixture (PL) consisting of PE, PG, and cardiolipin (molar ratio 81:17:2). In all experiments, the compartment to which peptide was added is named first (cis), and the compartment opposite to the addition (trans) was grounded. To be consistent with the literature, we used a negative sign for voltages if the potential applied to the cis-compartment is positive (i.e. reflecting a cell inside negative membrane potential). All measurements were performed in 5 mM Hepes, 100 mM KCl, 5 mM $MgCl_2$, pH 7.0 (specific electrical conductivity 17.2 mS/cm) at 37 °C. Representative current traces of at least five independent measurements are shown.

RESULTS

Solution structure of arenicin

In total, 194 distance restraints obtained by NMR spectroscopy were used to calculate the structure of arenicin. Table 2 summarizes the analysis of the ensemble representing the solution structure of arenicin. Arenicin is a two-stranded anti-parallel β-sheet (Cys3-Val10 and Val13-Cys20) stabilized by nine intra-backbone hydrogen bonds and a disulfide bond between Cys3 and Cys20 (Fig. 1A). The strands of the β-sheet are connected by a type I' β-turn. Arenicin shows an amphiphilic surface with distinct hydrophobic and hydrophilic areas.

The electrostatic potential surface of the averaged arenicin structure reveals large hydrophobic areas separated by the positively charged arginine side chains (Fig 1B). Since the charged arginine side chains are highly mobile, this picture reflects only a static image of the charge distribution. However, this characteristic distribution of charged and hydrophobic areas is achieved by inserting a significant right-handed twist into the β-sheet-structure, thus preventing an even charge distribution on the molecular surface. A comparison with the previously published structure of arenicin isoform 2 [24] revealed that, despite the right-handed twist, the β-sheet of the arenicin isoform 2 is almost planar whereas in case of the isoform 1 the β-sheet is bent. As a consequence, the overall shape of arenicin isoform 1 resembles a globular protein, thus contrasting with the elongated shape of the isoform 2.

Cytotoxic activity

The cytotoxicity of arenicin and two reference peptides, i.e. bee venom melittin and polymyxin B, was monitored by measuring the release of hemoglobin from freshly isolated human erythrocytes and by monitoring their effect on the metabolic activity of human Jurkat T-cells. Arenicin, in sharp contrast to the highly hemolytic melittin (LD_{50} = 3-4 µM), appeared to be only moderately lytic with an LD_{50} above 40 µM (35.5 % lysis at 30 µM). Notably, polymyxin B, despite its considerable hydrophobicity due to its alkyl chain, was completely non-hemolytic up to a concentration of 30 µM. Reduction of the incubation temperature from 37°C to 4°C did not abolish hemolysis, but led to a significantly reduced hemolytic effect of arenicin (9 % at 30 µM). By contrast, arenicin was substantially toxic to Jurkat cells. Killing was time- and concentration-dependent with an LD_{50} of 4, 3.5, and 2.7 µM at 37°C after 1, 2, and 3 h of incubation, respectively. For comparison, melittin was effective against Jurkat cells with an LD_{50} between 0.15 and 0.3 µM under the same conditions.

Antibacterial activity

We tested the antibacterial activities of the peptides under various buffer conditions using three deep-rough mutant (LPS Re chemotype) Gram-negative bacterial strains with well defined LPS structures (Fig. 1C, D), one of which we used in parallel for the preparation of model membranes to correlate biological with biophysical data. The bacterial panel includes human pathogens and laboratory strains. From the perspective of drug development, it was chosen to reflect strains which are in general more sensitive to the action of cationic peptides, i.e. *E. coli* WBB01, and strains which appear more resistant, in particular to the action of polymyxin B, the prototype of a cationic peptidic antibiotic with potent activity against Gram-negative bacteria, i.e. *Proteus mirabilis* R45. In addition, we tested the antibacterial activity of the peptides against two rough-mutant (LPS Ra chemotype) strains with LPS having complete core oligosaccharides.

Arenicin was active against all bacterial strains at similar low concentration and, among the peptides tested, it was the most potent one against *P. mirabilis* (Tab. 1).

Its activity was lower at a physiological salt concentration (150 mM) compared to buffer without any added salt. However, in buffers with varying ionic strength (150-500 mM), the activity of the peptide remained virtually constant. In particular the MIC of arenicin against *P. mirabilis* was very low, even under conditions where polymyxin B was completely inactive. The further addition of a bivalent cation (i.e. Mg^{2+}) was without any measurable effect. Notably, the arenicin concentration necessary to kill *E. coli* WBB01 and *P. mirabilis* R45 was the same at 37°C and at 4°C.

The kinetics of bacterial killing by arenicin is rapid, as assessed by plating out bacterial suspensions and colony counting after incubation with the peptide (Fig. 2). At 5 µM arenicin, complete killing of *E. coli* WBB01 was observed even after 5 min. It is worth mentioning that inhibitory and bactericidal concentrations which can be derived from these curves may differ from those shown in Table 1, as here bacteria were incubated in buffer alone to avoid growth during the incubation period. However, a substantial replication of bacteria was observed overnight even in buffer alone. This is in particular reflected in the case of *P. mirabilis* in the presence of 1 µM peptide (Fig. 2).

Ultrastucture of *E. coli* WBB01

The effect of arenicin (10 µM) on bacteria (exemplified here for *E. coli* WBB01) was visualized by atomic force and electron microscopy. For AFM measurements, bacteria were incubated with the peptide in LB medium. As depicted in Fig. 3, arenicin had a dramatic

impact on the structural integrity of bacteria when compared to an untreated control. For electron microscopy, bacteria were incubated alone and in the presence of the peptide for 30 min at 37°C in Hepes buffer supplemented with 10% LB medium (Fig. 4). Under these conditions, 79% of bacteria were killed. Apparent steps in arenicin-mediated killing of *E. coli* became visible at higher magnification (Fig. 4B), beginning with the formation of membrane blebs, release and condensation of cytoplasmic material, detachment of the outer membrane from the plasma membrane and formation of electron-dense spots on the outer membrane. Finally, the complete cytoplasm disappeared and the bacteria were covered with the spots which may represent aggregated lipopolysaccharide from the outer membrane. Interestingly, bacteria undergoing cell division always exhibited two cytoplasm clearing sites and the electron-dense spot formation was concentrated at the septum.

Permeabilisation of bacterial membranes

As the observed ultrastructure of arenicin-treated bacteria strongly suggested a membranolytic step in the mode of action of this peptide, we investigated the uptake of a DNA-intercalating dye, SYTOX green, by a suitable bacterial strain, i.e. *E. coli* D31, during incubation with arenicin. Dye uptake directly reflects membrane permeabilisation, as SYTOX green itself is not permeable through an intact lipid bilayer. In the case of Gram-negative bacteria, inner and outer membrane permeabilisation is apparently necessary to accomplish dye uptake. Considerable dye uptake was measurable even after 5 min of incubation of bacteria with the peptide (Fig. 5). The minimal inhibitory concentration of arenicin for *E. coli* D31, measured in parallel under these conditions, was 0.125 µM. Arenicin was also capable of permeabilizing the plasma membrane of a Gram-positive bacterial strain, *B. megaterium* (data not shown).

Circular dichroism (CD)

CD spectroscopy was used to study the conformation of arenicin bound to liposomes. Figure 6 shows the CD spectra of arenicin in the absence as well in the presence of PG liposomes. The CD spectrum of arenicin in solution shows the typical shape of a β-sheet peptide with a positive absorption band at 230 and a negative absorption band at 216 nm. This shape is dramatically changed in the presence of PG liposomes. The overall shape of the spectrum is indicative of a helical conformation of the peptide, although the two minima (219 and 231 nm) of the spectra are shifted to a higher wavelength compared to a CD spectrum of a helical protein in solution (208 and 222 nm). This shift indicates that arenicin inserts into the hydrophobic core of the PG liposomes and thereby undergoes a conformational change.

Insertion into model membranes

We used FRET spectroscopy as a sensitive tool to detect the specific interaction of arenicin with pure phospholipid and LPS bilayers. Binding and subsequent insertion of peptide into the lipid bilayer is assumed to result in an increase in membrane area and with that in fluorescent probe dilution and in an increase of the observed FRET signal. Liposomes composed of zwitterionic phosphatidylcholine (PC) and of negatively charged phosphatidylglycerol (PG) were chosen to mimic the plasma membranes of human cells and of bacteria, respectively. Aggregates made of LPS Re purified from *E. coli* strain WBB01 were used as a mimetic of the Gram-negative outer membrane. At 37 °C, rapid intercalation of arenicin was observed in all types of model membranes (Fig. 7). In the different lipid systems the changes in the FRET signal cannot be compared directly due to different aggregate structures. However, different intercalation characteristics were observed at lower temperatures as compared to 37 °C for the various lipids. An enhanced intercalation of peptide was observed particularly into the LPS membrane but also into the negatively charged PG membrane when compared to PC. By contrast, arenicin intercalation into zwitterionic PC liposomes was decreased at lower temperature.

Permeabilisation of model membranes

Addition of arenicin to asolectin liposomes, loaded with potassium and a fluorescent dye, led to the immediate dissipation of a valinomycin-induced membrane potential (Fig. 8), and was the first direct evidence for a pore-forming activity of the peptide. To further characterize the electrical and geometrical properties of the arenicin-induced membrane lesions or pores and to investigate the lipid specificity of the peptide-membrane interaction, we employed the Montal-Mueller planar lipid bilayer technique. This system allows the reconstitution of membranes with virtually any lipid composition, including symmetrical membranes of DPhyPC (Fig. 9A) and a defined phospholipid mixture (PL) mimicking roughly the plasma membrane of human cells and the cytoplasmic membrane of bacteria (Fig. 9B). Moreover, the asymmetrical outer membrane of the envelope of Gram-negative, consisting of LPS on its outer leaflet and PL on its inner leaflet could also be reconstituted (Fig. 9C). Upon addition of arenicin to the *cis* side of a planar lipid bilayer and setting of a negative trans-membrane voltage, we observed spontaneous current fluctuations after a certain lag period. The fluctuations appeared and vanished in a cooperative manner and reached conductivity levels of maximal 4 nS and a life time of several ms. The accumulation

of a number of lesions eventually led to a dramatic increase in current flow and the disruption of the membrane (arrow). Both conductivity and lifetime are indistinguishable in all three types of membranes suggesting in all cases the formation of structurally heterogeneous lesions rather than defined pores. Representative current traces are shown in Fig. 9A-C.

DISCUSSION

Arenicins are remarkably active effector molecules of the lugworm´s immune system and exhibit a broad spectrum antimicrobial activity [1]. These particular antimicrobial peptides (AMPs) caught our attention because of their unique cysteine-bridged large loop structure. Mechanistic information about how this new class of AMPs interacts with and kills bacteria has not been published so far. Arenicin isoform 1, which we have studied here in detail, forms a stable tertiary structure in solution, which resembles that of isoform 2 [24], though isoform 1 exhibits a more globular form when compared with the elongated structure of arenicin isoform 2. Detailed analyses of the structures revealed that the two isoforms do not differ significantly in their backbone-dihedral angles and that these are not responsible for the overall structural difference. The right handed twist in one of the β-strands in arenicin isoform 1 is due to experimentally derived ^{1}H-^{1}H distances that have not been observed in isoform 2 [24]. In addition, the bend of the arenicin isoform 1 β-sheet originates from observed long-range side chain contacts that also have not been described for the isoform 2. The anti-parallel β-sheet is twisted to expose an amphipathic surface. Other β-sheet AMPs, such as protegrin-1 and tachyplesin-1, adopt similar solution structures [25,26] though the β-sheet of arenicin is much more extended and is not caged between two disulfide bonds. This is in contrast to most α-helical AMPs, which only adopt a defined secondary structure upon interaction with membranes or membrane-mimetic environments [12,27]. As arenicin is amphipathic and rich in arginine and hydrophobic amino-acid residues, it is reasonable to suppose that disruption of the membrane is involved in killing of the bacteria. To address this hypothesis, we investigated its interactions with Gram-negative bacteria and model membranes. In our comprehensive studies on the antibacterial properties of arenicin, unequivocal evidence was found for the peptide-induced permeabilisation of the LPS-containing outer membrane and the phospholipid-containing cytoplasmic membrane of bacteria. Killing of *E. coli* and of polymyxin B-resistant *P. mirabilis* occurred within minutes and the ultrastructural analyses of arenicin-treated *E. coli* revealed signs of cell envelope destruction. Accordingly, the permeabilisation of both membranes of viable *E. coli* also occurred within minutes. No pronounced lipid specificity for intercalation and pore formation of arenicin in model membranes composed to mimic the respective biological targets (i.e. zwitterionic PC for the erythrocyte plasma membrane, negatively charged PG or a phospholipid mixture of PG, cardiolipin, and of zwitterionic phosphatidylethanolamine for the bacterial cytoplasmic

membrane, and of LPS for the outer membrane of Gram-negative bacteria, such as *E. coli*, *S. enterica*, and *P. mirabilis*) was observed. This is in contrast to the situation with other AMPs, such as polymyxin B and human β-defensin 3 for which the LPS structure, in particular the distribution of negatively charged groups, was decisive for the antibacterial activity [23,28].

Arenicin-induced permeabilisation of model membranes is accompanied by peptide intercalation into the bilayer and a transmembrane current flow characteristic for structurally heterogeneous lesions. At a first glance, the characteristics of the obtained current fluctuations in planar lipid bilayers may fit into the carpet model [29] rather than to a barrel-stave pore with defined geometry [30]. However, in general this view may be oversimplified [31].

How does the structure of arenicin fit into the experimentally observed characteristics of the membrane lesions? Oligomerization of β-sheet domains is well docomented for bacterial pore-forming toxins, such as α-toxin from *Staphylococcus aureus*. However, membrane pores formed by these toxins have a highly ordered cylindrical geometry [32]. Apparently, arenicin undergoes a pronounced conformational change after insertion into a membrane. Since it is too short to span an entire bilayer it may be speculated that membrane defects were only elicited in the *cis* monolayer which could explain the heterogenicity of the observed lesions. Further studies will shed more light on this issue.

The concentration of arenicin effective in killing bacteria was almost identical to the concentration that induced measurable effects on the respective model membranes. Although this does not rule out potential intracellular targets, it implies that membrane interaction, if it is not the lethal event itself, is at least an essential step in bacterial killing. This is in concordance with recent data, where we have shown that the interaction of various AMPs with model membranes of lipid compositions resembling those of different target cells, reflected their biological activity [12,23,33].

The main focus of this study is the interaction of arenicin with Gram-negative bacteria and respective biomembrane mimetics. However, we would expect comparable results with Gram-positive bacteria and this has been proven exemplarily for membrane permeabilisation of *B. megaterium*. The broader target cell selectivity of arenicin compared to other AMPs, reflected in particular in a considerable cytotoxicity against Jurkat cells, may be attributed to the high salt concentration of the natural habitat of the lugworm. As the selectivity of peptides is mainly based on electrostatic interactions of the cationic peptide with the negatively charged bacterial surface [33,34], this interaction is impaired at the high salt concentration found in sea water and thus a more pronounced hydrophobic interaction, which is presumably responsible for cytotoxicity, is necessary to guarantee a potent antimicrobial activity. The

evolutionary selection of arginines instead of lysines may also be an adaptation to high salt environment. It has been recently published that a lysine derivative of human α-defensin-1 is much less active and has a higher sensitivity to increasing salt concentration than the arginine-containing wild-type molecule [35].

In summary, we have elucidated the structure and mode of action of arenicin isoform 1, a representative of a new class of AMPs. The peptide folds into a defined β-sheet tertiary structure and permeabilizes bacterial membranes which is a key step in bacterial killing. Its potent activity against polymyxin B resistant *P. mirabilis*, even at high ionic strength, its short length, and disulfide-bond stabilized tertiary structure make arenicin a particularly interesting antimicrobial compound and a lead structure for antibiotic drug development.

Acknowledgements

We thank Annemarie Brauser for taken AFM images, Dr. Christoph Gelhaus for performing mass spectrometry, Christine Hamann for FRET measurements, Heike Kühl for electron microscopy, Christoph Lemke for measurements on planar lipid bilayers, Kerstin Stephan for antibacterial testings, and Dr. Lee Shaw for critical reading of the manuscript. This study has been carried out with financial support from the Deutsche Forschungsgemeinschaft (SFB 617 ´Molecular mechanisms of epithelial defense´, projects A9, A17, and A18). A.K. was supported by a short-term fellowship of the SFB 617 during her stay in Kiel, Germany.

REFERENCES

1 Ovchinnikova, T. V., Aleshina, G. M., Balandin, S. V., Krasnosdembskaya, A. D., Markelov, M. L., Frolova, E. I., Leonova, Y. F., Tagaev, A. A., Krasnodembsky, E. G. and Kokryakov, V. N. (2004) Purification and primary structure of two isoforms of arenicin, a novel antimicrobial peptide from marine polychaeta *Arenicola marina*. FEBS Lett. **577**, 209-214

2 Zasloff, M. (2002) Antimicrobial peptides of multicellular organisms. Nature **415**, 389-395

3 Devine, D. A. and Hancock, R. E. W., eds. (2004). Mammalian host defense peptides, Cambridge University Press, Cambridge

4 Ganz, T., Selsted, M. E., Szklarek, D., Harwig, S. S., Daher, K., Bainton, D. F. and Lehrer, R. I. (1985) Defensins. Natural peptide antibiotics of human neutrophils. J. Clin. Invest. **76**, 1427-1435

5 Bruhn, H., Winkelmann, J., Andersen, C., Andrä, J. and Leippe, M. (2006) Dissection of the mechanisms of cytolytic and antibacterial activity of lysenin, a defence protein of the annelid *Eisenia fetida*. Dev. Comp. Immunol. **30**, 597-606

6 Harder, J., Bartels, J., Christophers, E. and Schröder, J. M. (1997) A peptide antibiotic from human skin. Nature **387**, 861

7 Harder, J., Bartels, J., Christophers, E. and Schröder, J. M. (2001) Isolation and characterization of human beta-defensin-3, a novel human inducible peptide antibiotic. J. Biol. Chem. **276**, 5707-5713

8 Laube, D. M., Yim, S., Ryan, L. K., Kisich, K. O. and Diamond, G. (2006) Antimicrobial peptides in the airway. Curr. Top. Microbiol. Immunol. **306**, 153-182

9 Zasloff, M. (1987) Magainins, a class of antimicrobial peptides from *Xenopus* skin: Isolation, characterization of two active forms, and partial cDNA sequence of a precursor. Proc. Natl. Acad. Sci. USA **84**, 5449-5453

10 Boman, H. G. (1991) Antibacterial peptides: key components needed in immunity. Cell **65**, 205-207

11 Lehrer, R. I., Ganz, T. and Selsted, M. E. (1991) Defensins: endogenous antibiotic peptides of animal cells. Cell **64**, 229-230

12 Andrä, J., Monreal, D., Martinez de Tejada, G., Olak, C., Brezesinski, G., Sanchez Gomez, S., Goldmann, T., Bartels, R., Brandenburg, K. and Moriyon, I. (2007) Rationale for the design of shortened derivatives of the NK-lysin derived antimicrobial peptide NK-2 with improved activity against Gram-negative pathogens. J. Biol. Chem. **282**, 14719-14728

13 Boman, H. G., Nilsson-Faye, I., Paul, K. and T. Rasmuson, J. (1974) Insect immunity. I. Characteristics of an inducible cell-free antibacterial reaction in hemolymph of *Samia cynthia* pupae. Infect. Immun. **10**, 136-145

14 Galanos, C., Lüderitz, O. and Westphal, O. (1969) A new method for the extraction of R lipopolysaccharides. Eur. J. Biochem. **9**, 245-249

15 Guntert, P., Mumenthaler, C. and Wüthrich, K. (1997) Torsion angle dynamics for NMR structure calculation with the new program DYANA. J. Mol. Biol. **273**, 283-298

16 Kraulis, P. J. (1991) MOLSCRIPT: a program to produce both detailed and schematic plots of protein structures. J. Appl. Crystallography **24**, 946-950

17 Nicholls, A., Sharp, K. A. and Honig, B. (1991) Protein folding and association: insights from the interfacial and thermodynamic properties of hydrocarbons. Proteins **11**, 281-296

18 Chen, G. C. and Yang, Y. T. (1977) Two-point calibration of circular dichrometer with d-10-camphorsulfonic acid. Anal. Lett. **10**, 1195-1207

19 Schromm, A. B., Brandenburg, K., Rietschel, E. T., Flad, H. D., Carroll, S. F. and Seydel, U. (1996) Lipopolysaccharide-binding protein mediates CD14-independent intercalation of lipopolysaccharide into phospholipid membranes. FEBS Lett. **399**, 267-271

20 Leippe, M., Ebel, S., Schoenberger, O. L., Horstmann, R. D. and Müller-Eberhard, H. J. (1991) Pore-forming peptide of pathogenic *Entamoeba histolytica*. Proc. Natl. Acad. Sci. USA **88**, 7659-7663

21 Montal, M. and Mueller, P. (1972) Formation of bimolecular membranes from lipid monolayers and a study of their electrical properties. Proc. Natl. Acad. Sci. USA **69**, 3561-3566

22 Wiese, A. and Seydel, U. (2000) Electrophysiological measurements on reconstituted outer membranes. Methods Mol. Biol. **145**, 355-370

23 Böhling, A., Hagge, S. O., Roes, S., Podschun, R., Sahly, H., Harder, J., Schröder, J. M., Grötzinger, J., Seydel, U. and Gutsmann, T. (2006) Lipid-specific membrane activity of human beta-defensin-3. Biochemistry **45**, 5663-5670

24 Ovchinnikova, T. V., Shenkareva, Z. O., Nadezhdina, K. D., Balandina, S. V., Zhmaka, M. N., Kudelinaa, I. A., Finkinaa, E. I., Kokryakovb, V. N. and Arseniev, A. S. (2007) Recombinant expression, synthesis, purification, and solution structure of arenicin. Biochem. Biophys. Res. Comm. **360**, 156-162

25 Fahrner, R. L., Dieckmann, T., Harwig, S. S., Lehrer, R. I., Eisenberg, D. and Feigon, J. (1996) Solution structure of protegrin-1, a broad-spectrum antimicrobial peptide from porcine leukocytes. Chem. Biol. 3, 543-550

26 Laederach, A., Andreotti, A. H. and Fulton, D. B. (2002) Solution and micelle-bound structures of tachyplesin I and its active aromatic linear derivatives. Biochemistry **41**, 12359-12368

27 DeGrado, W. F. and Lear, J. D. (1985) Induction of peptide conformation at apolar/water interfaces. 1. A study with model peptides of defined hydrophobic periodicity. J. Am. Chem. Soc. **107**, 7684-7689

28 Wiese, A., Münstermann, M., Gutsmann, T., Lindner, B., Kawahara, K., Zähringer, U. and Seydel, U. (1998) Molecular mechanisms of polymyxin B-membrane interactions: direct correlation between surface charge density and self-promoted transport. J. Membr. Biol. **162**, 127-138

29 Oren, Z. and Shai, Y. (1998) Mode of action of linear amphipathic α-helical antimicrobial peptides. Biopolymers **47**, 451-463

30 Boheim, G. J. (1974) Statistical analysis of alamethicin channels black lipid membranes. J. Membr. Biol. **19**, 277-303

31 Bechinger, B. and Lohner, K. (2006) Detergent-like actions of linear amphipathic cationic antimicrobial peptides. Biochim. Biophys. Acta **1758**, 1529-1539

32 Song, L., Hobaugh, M. R., Shustak, C., Cheley, S., Bayley, H. and Gouaux, J. E. (1996) Structure of staphylococcal alpha-hemolysin, a heptameric transmembrane pore. Science **274**, 1859-1866

33 Schröder-Borm, H., Willumeit, R., Brandenburg, K. and Andrä, J. (2003) Molecular basis for membrane selectivity of NK-2, a potent peptide antibiotic derived from NK-lysin. Biochim. Biophys. Acta **1612**, 164-171

34 Matsuzaki, K., Sugishita, K., Fujii, N. and Miyajima, K. (1995) Molecular basis for membrane selectivity of an antimicrobial peptide, magainin 2. Biochemistry **34**, 3423-3429

35 Zou, G., de Leeuw, E., Li, C., Pazgier, M., Zeng, P., Lu, W. Y., Lubkowski, J. and Lu, W. (2007) Toward understanding the cationicity of defensins. Arg and Lys versus their noncoded analogs. J. Biol. Chem. **282**, 19653-19665

Figure legends

Fig. 1

Ribbon representation of the three-dimensional structure (A) and the electrostatic potential map of arenicin (B). Both structures are shown in an identical orientation. Positively charged regions are depicted in blue. The structure has been deposited in the RCSB protein data base (PDB ID: 2JSB). Structures of LPS from the various deep rough mutant bacterial strains used in this study are illustrated schematically (C). LPS isolated from *E. coli* WBB01, *S. enterica* R595 and *P. mirabilis* R45 differ mainly in the degree of aminoarabinose (Ara4N) substitutions at 4´- and 1-phosphate of the diglucosamine backbone of the lipid A moiety (R1) and at the carboxyl group of the first Kdo sugar (R2) [28]. The position of the Ara4N R1-substitution cannot be assigned to either phosphate group. Non-stoicheiometric Ara4N substitutions of LPS, and net charges are listed in (D).

Fig. 2

Time course of bacterial killing by arenicin. Bacteria (*E. coli* WBB01 and *P. mirabilis* R45) were incubated alone (control) and in the presence of three different concentrations of arenicin in buffer (20 mM Hepes, 150 mM NaCl, pH 7.0) at 37°C. Viability of bacteria was assessed by plating out the bacterial suspensions at various time points and is presented as CFU (% of control) = ($CFU_{peptide}$ / $CFU_{control}$) * 100.

Fig. 3

Effect of arenicin treatment on the morphology of bacteria (I). AFM images of an untreated *E. coli* WBB01 (A) and of one incubated with 10 µM arenicin (B) in LB medium at 37°C for 30 min. Images were taken in air in AC (tapping) mode. Length (bar) and height (colour code) scales are indicated.

Fig. 4

Effect of arenicin treatment on the morphology of bacteria (II). Transmission electron microscopy of untreated *E . coli* WBB01 (A, control) and of those incubated with 10 µM arenicin (A, + Arenicin) at 37°C for 30 min. Selected higher magnification pictures of bacteria incubated with the peptide are shown in B. Length scale: each bar represents 1 µm.

Fig. 5

Permeabilisation of bacterial membranes by arenicin. Damage of the outer and inner membrane of *E. coli* D31 induced by arenicin incubated for 5, 30, and 60 min was monitored via the uptake of the DNA-intercalating fluorescent dye SYTOX green.

Fig. 6

CD spectroscopy. The CD spectrum of arenicin in 50 mM sodium phosphate, pH 5.2 (solid line) and in the presence of PG liposomes (dashed line) is shown.

Fig. 7

Intercalation of arenicin into liposome membranes. Peptide intercalation into PC (A), PG (B) liposomes, and *E. coli* WBB01 LPS aggregates (C) was measured at three different temperatures by FRET spectroscopy. An increase of the FRET-signal ($I_{Donor}/I_{Acceptor}$) corresponds to a reduced FRET efficiency by dye dilution and is indicative for membrane insertion of the peptide.

Fig. 8

Permeabilisation of liposomes by arenicin. Addition of peptide (0.1 nmol) led to the immediate dissipation of a valinomycin-induced membrane potential in phospholipid vesicles (1 ml cuvette buffer, pH 7.5) and concomitantly to dequenching of the fluorescent dye. Grey areas indicate time periods at which the spectrofluorometer shutter was temporarily closed to enable compound addition (arrows).

Fig. 9

Permeabilisation of planar lipid membranes by arenicin. Time courses of peptide-induced current traces are shown for symmetrical DPhyPC (A), for PL membranes (B), and for an asymmetrical *E. coli* WBB01 LPS Re / PL membrane (C). The final peptide concentrations and the applied voltages were 0.7 µM / –100 mV (A), 0.5 µM / -20 mV (B), and 0.8 µM / -52 mV (C), respectively. An arrow indicates disruption of the respective membrane. Bar represents 100 ms, all traces are displayed using the same time scale.

Table 1 - Antibacterial activity of arenicin compared to that of melittin and polymyxin B against three deep rough (LPS Re) and two rough (LPS Ra) mutant bacterial strains at various buffer conditions: (1) 20 mM Hepes, pH 7.0; (2) 20 mM Hepes, 150 mM NaCl, pH 7.0; (3) 20 mM Hepes, 300 mM NaCl, pH 7.0; (4) 20 mM Hepes, 500 mM NaCl, pH 7.0; (5) 5 mM Hepes, 100 mM KCl, pH 7.0; (6) 5 mM Hepes, 100 mM KCl, 5 mM $MgCl_2$, pH 7.0; (7) PBS, pH 7.4. The minimal inhibitory concentration (MIC) and the minimal bactericidal concentration (MBC, in brackets) are given in µM. The assay was performed in 10 % LB / 90 % buffer at 37°C and 4°C (when indicated). *, bacterial killing is not complete but >90 % at indicated concentration; n.a., not accomplishable; n.d., not done.

Strain	LPS	Buffer / T	Salt conc. (M)	Arenicin	Melittin	Polymyxin B
E. coli WBB01	Re	1	0	0.3 (0.6)	0.6 (2.5)	0.15 (0.6)
		1 / 4°C	0	n.a. (0.6)	n.d.	n.d.
		2	0.15	1.25 (2.5)	2.5 (5)	1.25 (1.25)
		3	0.3	2.5 (5)	40 (40)	1.25 (2.5)
		4	0.5	2.5 (5)	40 (>40)	1.25 (5)
		5	0.1	1.25 (2.5)	1.25 (1.25)	0.6 (2.5)
		6	0.1	1.25 (5)	5 (10)	1.25 (2.5)
		7	0.15	1.25 (5)	1.25 (1.25)	1.25 (1.25)
P. mirabilis R45	Re	1	0	0.6 (2.5)	2.5 (10)	0.6 (5)
		1 / 4°C	0	n.a. (2.5)	n.d.	n.d.
		2	0.15	5 (20*)	20 (>40*)	>40 (>40)
		3	0.3	5 (20*)	>40 (>40)	>40 (>40)
		4	0.5	5 (20*)	>40 (>40)	>40 (>40)
		5	0.1	5 (20)	20 (40*)	> 40 (>40)
		6	0.1	2.5 (>10)	40 (40)	> 40 (>40)
		7	0.15	5 (20*)	20 (40)	> 40 (>40)
S. enterica R595	Re	1	0	0.6 (1.25)	0.6 (1.25)	0.3 (0.3)
		2	0.15	1.25 (2.5)	2.5 (5)	0.3 (0.3)
S. enterica R60	Ra	1	0	1.25 (2.5)	2.5 (5)	0.3 (0.3)
E. coli ATCC 23716	Ra	1	0	0.6 (0.6)	5 (10)	1.25 (1.25)

Table 2

Structural statistics for the 20 conformers of arenicin 1. No NOE distance restraint was violated by more than 0.5 Å in any of the structures.

Distance restraints[a]	
Intraresidue (i-j = 0)	111
Sequential (|i-j| = 1)	41
Medium range (2 ≤ |i-j| ≤ 4)	2
Long range (|i-j| ≤ 5)	16
Hydrogen bonds	9*2
Disulfide bonds	2*3
All	194
Average r.m.s.d.[b] **to mean in Å**	
Average backbone r.m.s.d. to mean	0.66 ± 0.27
Average heavy atom r.m.s.d. to mean	1.51± 0.26
Average r.m.s.d. to mean for secondary structures[c] **in Å**	
Average backbone r.m.s.d. to mean	0.45 ± 0.16
Average heavy atom r.m.s.d. to mean	1.34 ± 0.22

[a] Only the number of upper distance restraints is given; to each upper distance restraint corresponds one lower distance restraint.

[b] r.m.s.d. root mean square deviation.

[c] Residues 3 - 10, 13 – 20.

Biochemical Journal Immediate Publication. Published on 15 Oct 2007 as manuscript BJ20071051

A

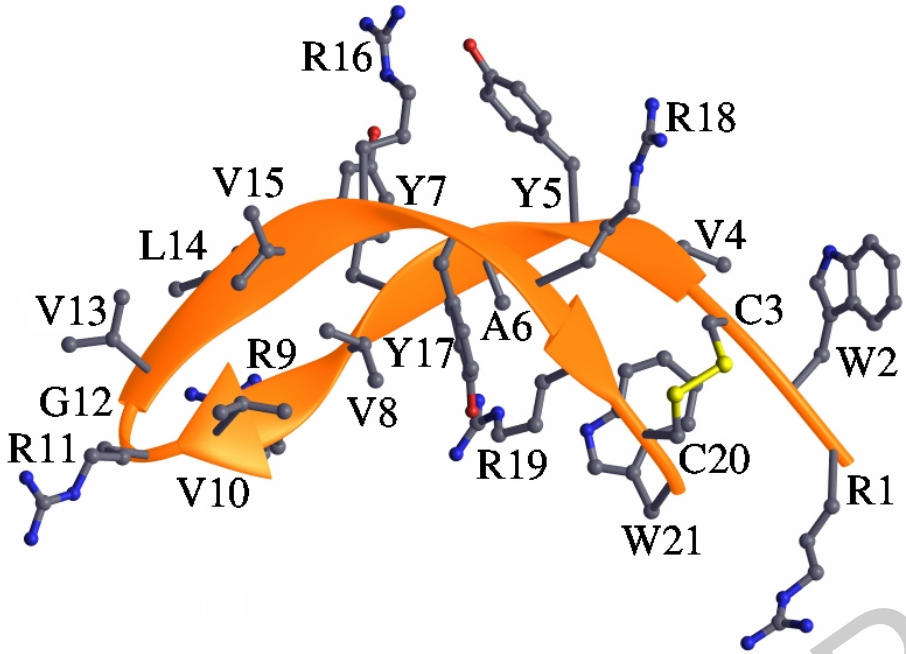

B

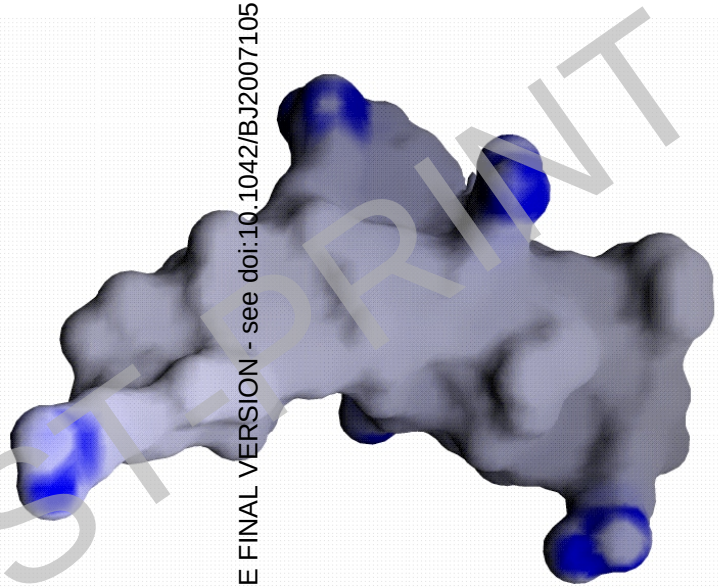

C

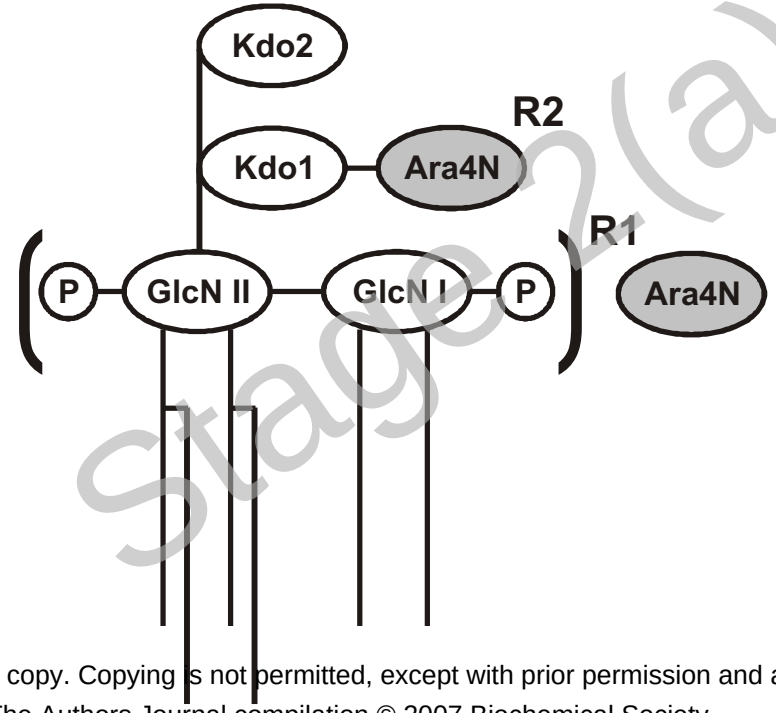

D

	LPS WBB01	LPS R595	LPS R45
R1	0 %	65 %	50 %
R2	0 %	0 %	50 %
Charge / e_0	-4	-3.4	-3

Biochemical Journal Immediate Publication. Published on 15 Oct 2007 as manuscript BJ20071051

Figure 2

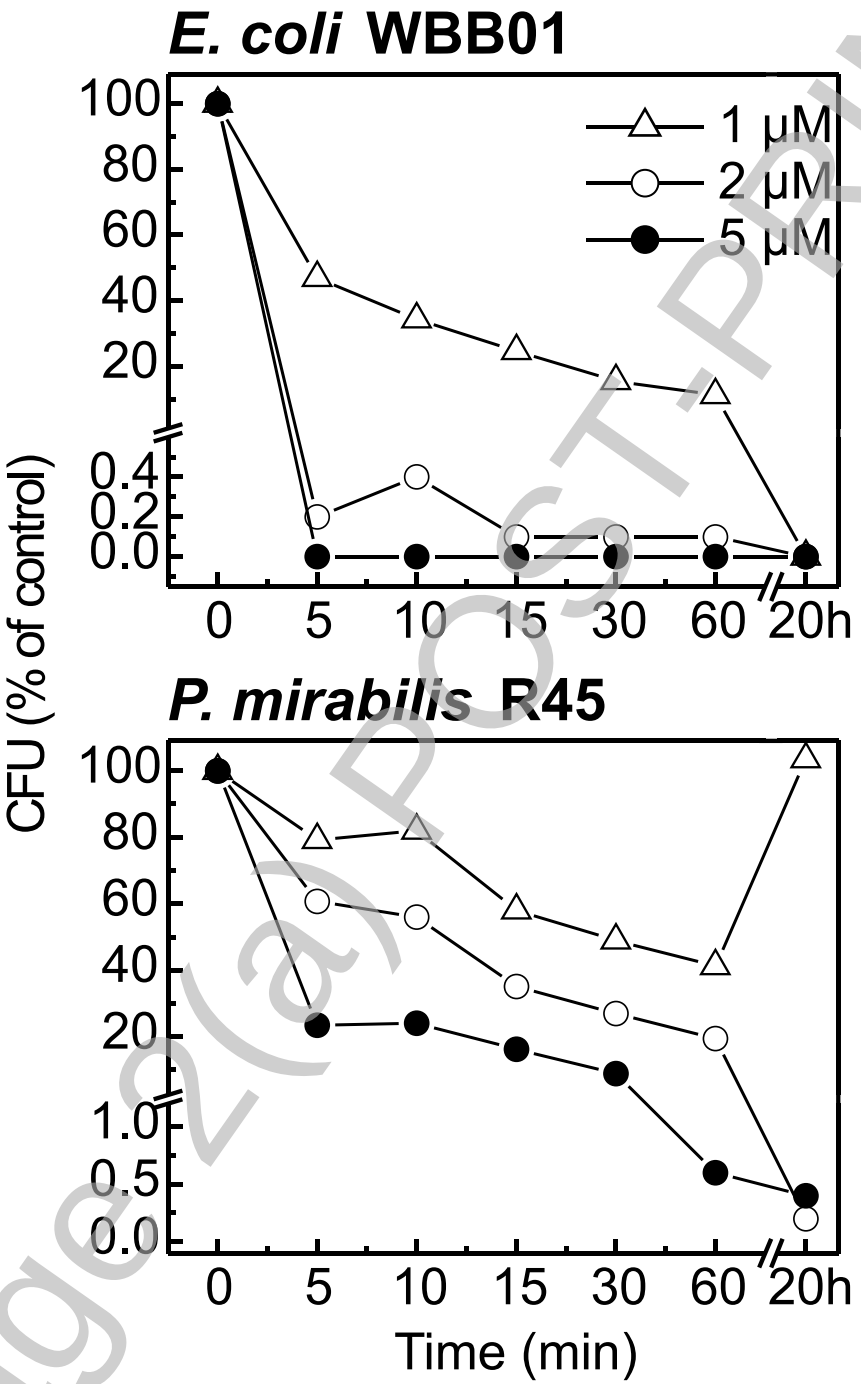

Biochemical Journal Immediate Publication. Published on 15 Oct 2007 as manuscript BJ20071051

Figure 3

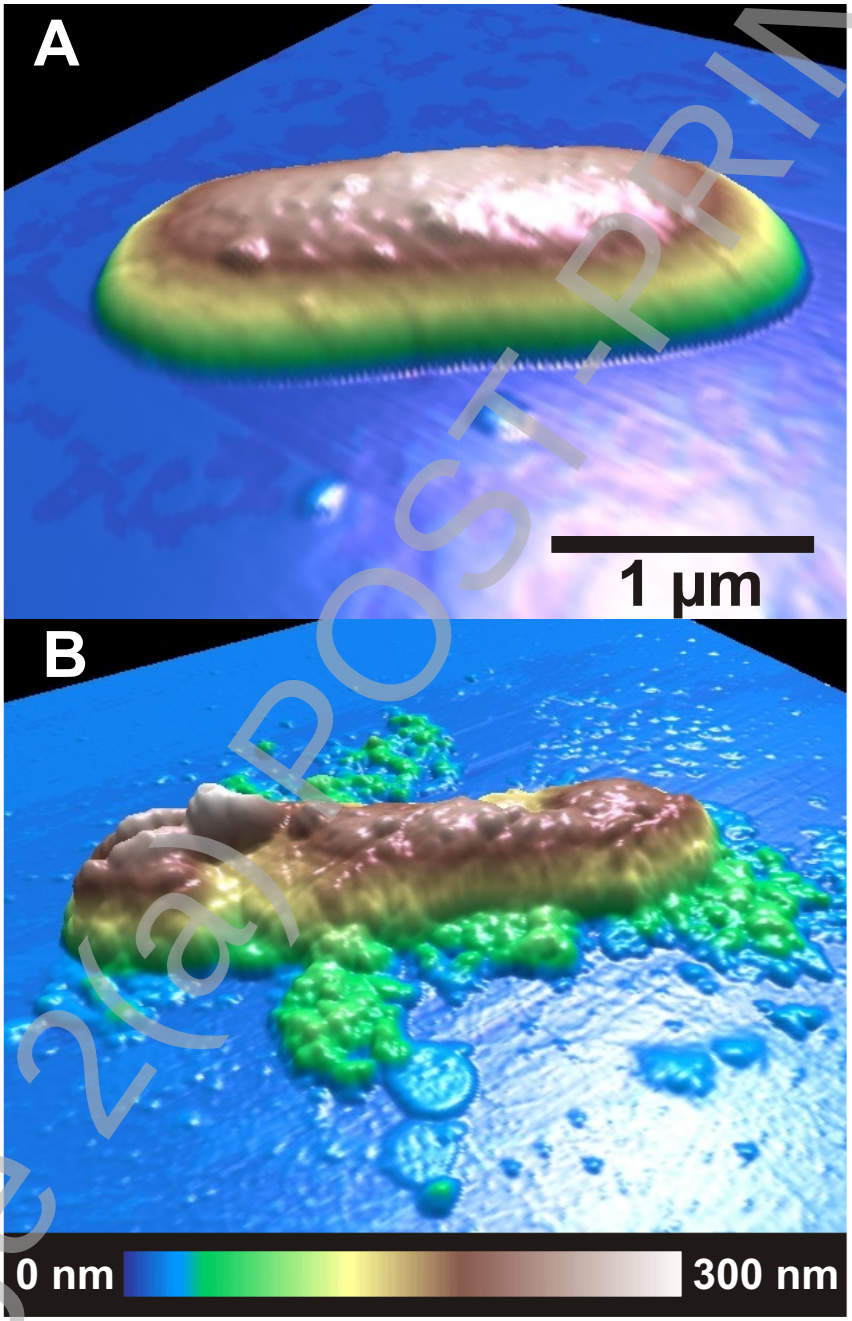

Biochemical Journal Immediate Publication. Published on 15 Oct 2007 as manuscript BJ20071051

Figure 4

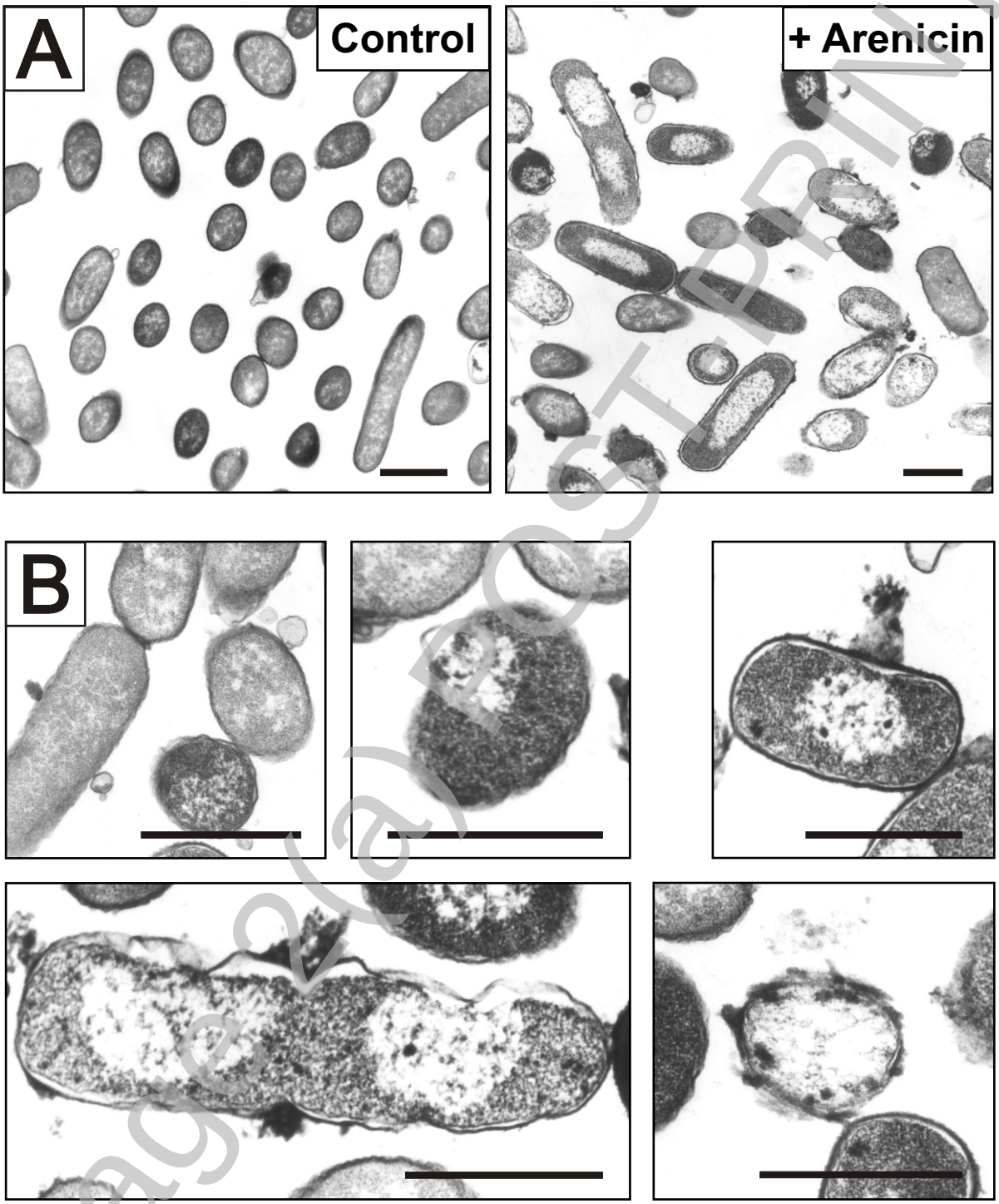

Biochemical Journal Immediate Publication. Published on 15 Oct 2007 as manuscript BJ20071051

Figure 5

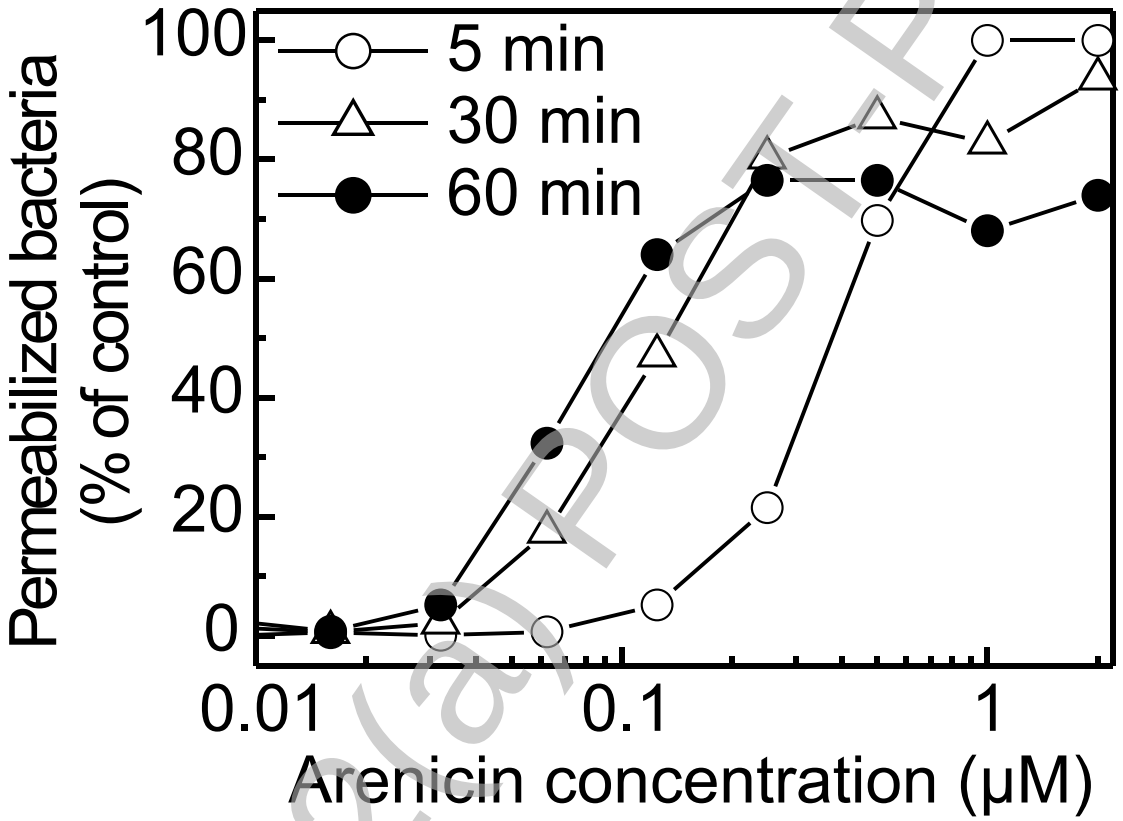

Figure 6

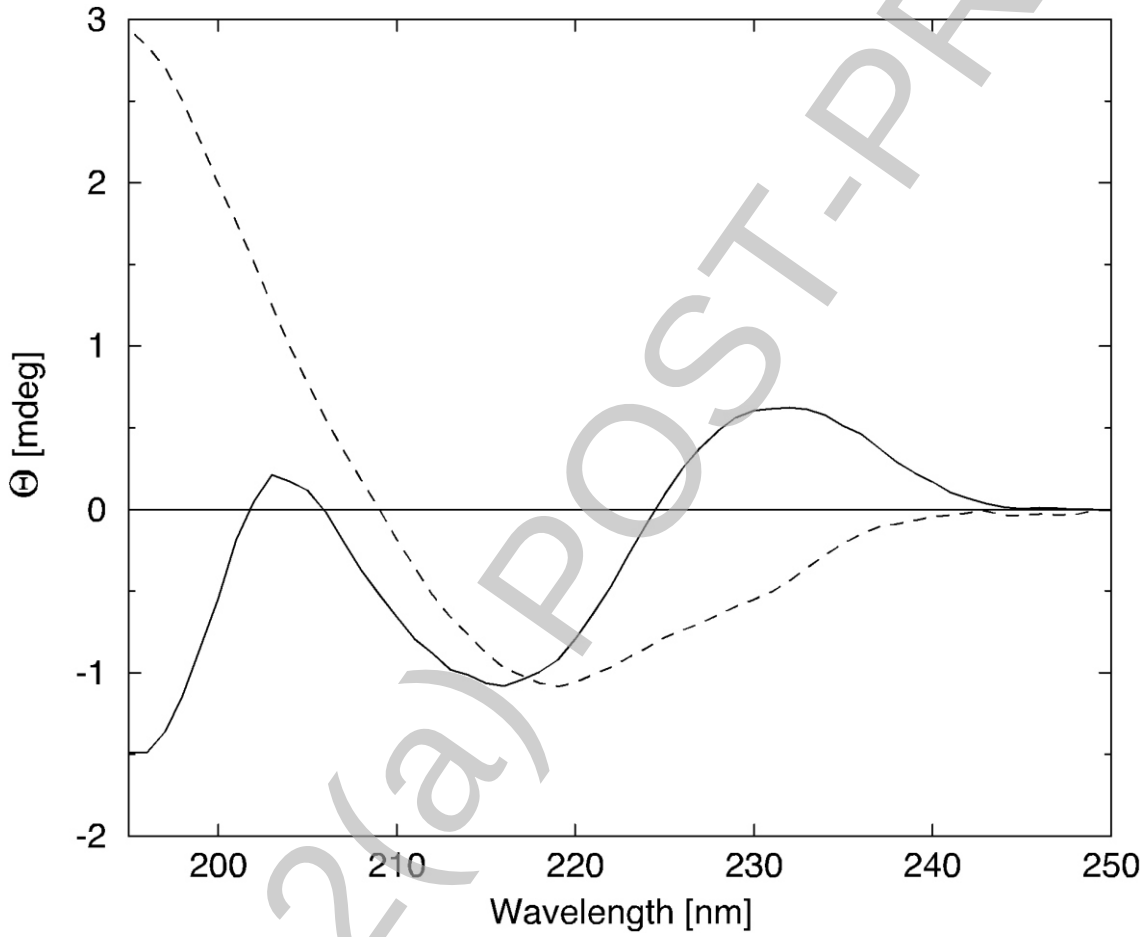

Biochemical Journal Immediate Publication. Published on 15 Oct 2007 as manuscript BJ20071051

Figure 7

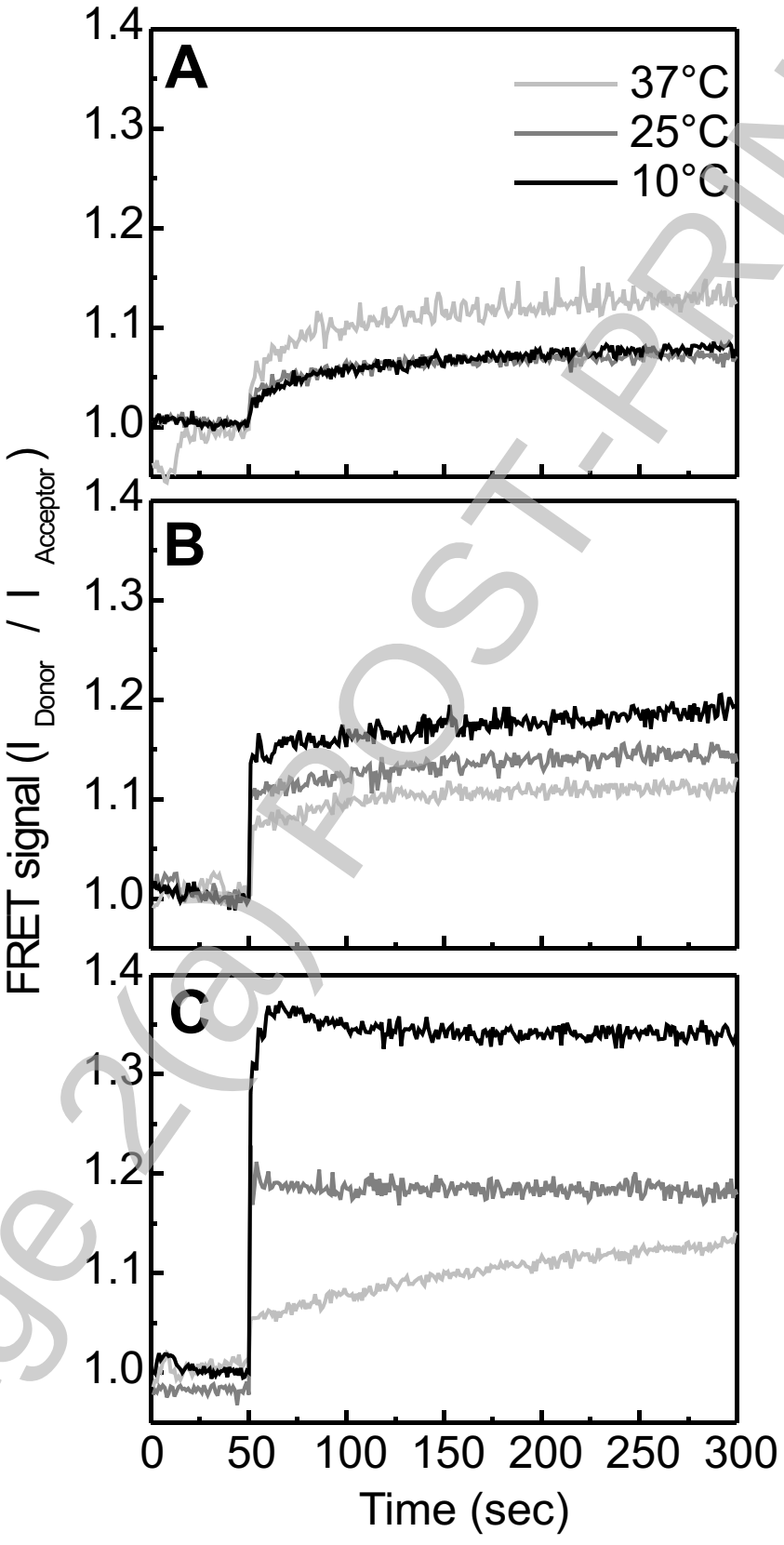

Biochemical Journal Immediate Publication. Published on 15 Oct 2007 as manuscript BJ20071051

Figure 8

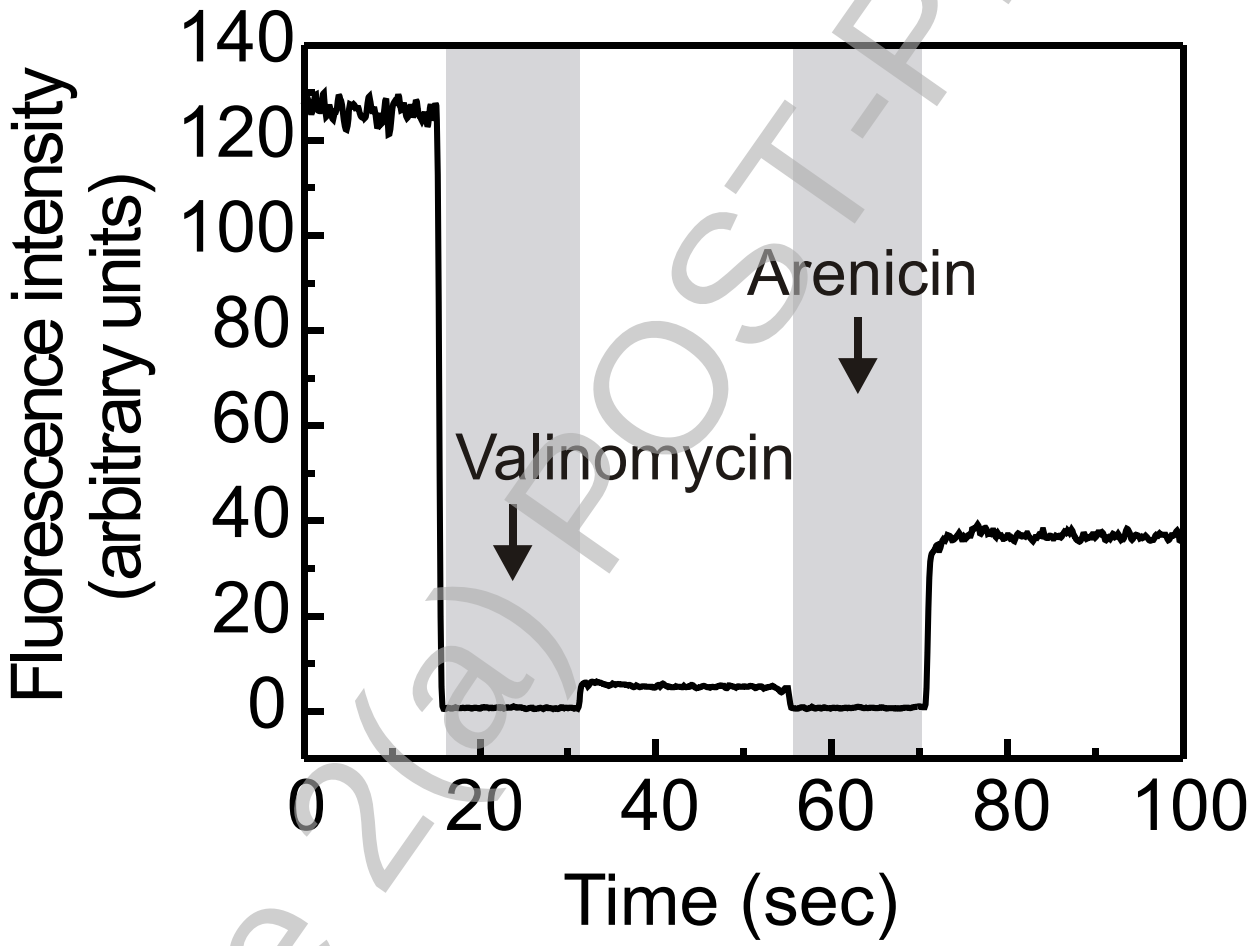

Biochemical Journal Immediate Publication. Published on 15 Oct 2007 as manuscript BJ20071051

Figure 9